Speed ripple and dead zone effects reduction in an 8/6 switched reluctance motor based on classical control strategies

J. D. GONZÁLEZ-SAN ROMÁN, J. U. LICEAGA-CASTRO, I. I. SILLER-ALCALÁ AND R. A ALCANTARA RAMIREZ
Department of Electronic
Universidad Autónoma Metropolitana-Azcapotzalco
Av. San Pablo Xalpa 180, Reynosa Tamaulipas, Azcapotzalco, C.P. 02200 Ciudad de México
MÉXICO

Abstract: - This work presents two control strategies, with the objective of reducing the undesirable effects of ripple and dead zone in the speed response of a switched reluctance motor (SRM) 8/6. The first strategy aims to reduce the dead zone by applying a double integrator classical controller, while the second strategy proposes a new strategy to reduce the speed ripple, which works in conjunction with a classic PI controller. The strategy, based on digital simulations shows a reduction on the dead zone effect and speed ripple, the simulations were performed using the Matlab® / Simulink software and are based on a simplified non-linear model that has the non-linearity of Coulomb friction plus viscous friction, as well as an ideal inverter circuit.

Key-Words: - Switched reluctance motor (SRM), speed control, PI controller, PII controller, PI+ Ripple Reductor controller, Linear control.

Received: April 7, 2021. Revised: September 26, 2021. Accepted: October 10, 2021. Published: October 23, 2021.

1 Introduction

As can be corroborated in different research works [1]-[5], switched reluctance motors have several interesting features or advantages, such as, simple and robust construction, high torque at low speeds, efficient energy conversion, large power-to-size ratio, easy cooling, and wide operating speed range.

For this reason, it is desirable to be able to use this type of motor making the most of each of these advantages. However, to be able to do this you need to meet two important requirements. The first is to optimally drive the motor with an inverter circuit, which ensures the independence of each of the phases and can demagnetize the active phases. The second requirement is to implement a control technique that allows reaching the desired position or speed efficiently.

This last point has prompted researchers to develop various control techniques for SRMs, which have different purposes. Some examples of these techniques are direct control of instantaneous torque [6] and [7], vector control [8] and [9], fuzzy logic control [10] and [11], among many others. However, most of the previous techniques can become very complex and difficult to implement, therefore, in the industry it is preferred to use classic controllers such as PI, due to its easy implementation, effectiveness and price. For this reason, much of the current research on the control of this type of motors seeks to improve this controller or design new control techniques taking the PI controller as a reference framework [12], [13] and [14].

One of the main problems to be solved through the control of the SRM's is undoubtedly to eliminate or reduce the ripple that appears naturally in the speed and torque responses. On the other hand, an improvement to be made in the operation of some direct current motors is the reduction of the dead zone, which, as occurs with ripple, affects the performance of the motor at low speeds.

In this work, two control techniques are presented, the objective of which is to eliminate or reduce the two problems described above. For this, the article is organized as follows:

Section 2 shows the electrical and mechanical characteristics of the motor, which were used to program the SRM simulations, as well as the transfer function and a PI controller that was tested on this motor. Later, in section 3 a PII controller is designed and simulated to address the dead zone problem of the SRM. In section 4, a PI control plus a ripple reductor is proposed, designed and simulated, which aims to reduce speed and torque oscillations. Finally, the section presents the conclusions of the work.

2 Characteristics and transfer function of the SRM 8/6

The parameters used for the development of this work are taken from the motor with eight stator poles and six rotor poles model RA130135 from the manufacturer System Tech, which are listed below [15]:

- $Vmax$ =24 Vdc
- $N = 4$
- $N_r = 6$
- $J = 3.9063$ Kg m^2
- $\tau_l = 0.01$ N m
- $D = 0.0001$ N m/rad/s
- $\Delta = 0.005$ N m
- $R = 1\ \Omega$
- $L_0 = 2.1$ mH
- $L_1 = 1.3$ mH

Through an analysis of the non-linear structure of the motor model (degree, relative degree and zero dynamics) and a subsequent linearization at an operating point, the single-phase transfer function of the motor is (1), as can be verified on [15].

$$G(s) = \frac{283470}{s^2 + 1619.7s + 6740.2} \tag{1}$$

Due to the wide distance between the two poles of the transfer function (1), it is possible to simplify it by means of pole dominance [16], obtaining the transfer function shown in (2).

$$G(s) = \frac{176.64}{s + 4.2} \tag{2}$$

As demonstrated in [17] this type of motor is easily controllable by a PI controller, satisfying robustness margins greater than the typical margins of 12dB of gain and 45 ° of phase, the transfer function and Bode diagram of said controller are shown in (3) and Fig. 1.

$$C(s) = \frac{0.0474(s + 4)}{s} \tag{3}$$

However, this controller exhibited the following two problems. Firstly, when operating at low speeds, approximately below 600rpm, motor performance was affected by dead zone non-linearity, causing starting difficulties and overshoots due to large increases in control input voltage. that the PI controller applied to the motor to get out of the dead zone.

The second problem that the control of this motor showed, was the ripple of the speed and torque signals, which are proven by the commutations of the motor, like the first problem, the ripple represents a problem for the user mainly to low speeds where the percentage of ripple can rise significantly.

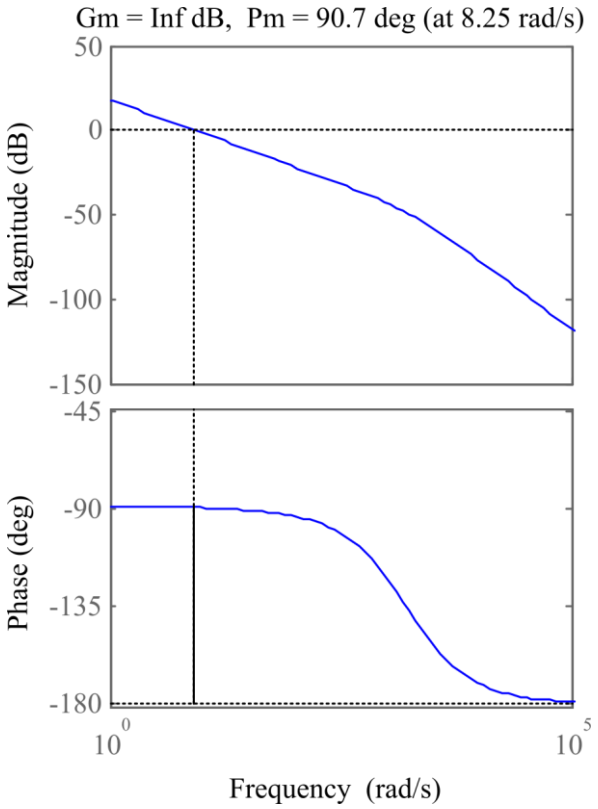

Fig. 1. PI Control system Bode diagram.

3 Proposed PII Controller

As demonstrated in [17] the PI controllers applied to SRM 8/6, it proved to have excellent performance in regulation and tracking, satisfying robust margins. However, as with other electric motors, the non-linear phenomenon called dead zone occurs, making it difficult to operate the motor at low speeds with the same performance. For this reason, in this section a proportional controller with double integral effect or PII is design, which, as demonstrated in [18], can minimize the dead zone effect.

The technique to design this controller is through Bode shaping, in this case we start from the already designed PI controller and add an integrator or pole at 0, a zero at low frequency to raise the phase and guarantee this margin, finally the gain is adjusted to get the desired bandwidth. The resulting transfer function for the PII controller is shown in (4).

$$C(s) = \frac{0.057828(s + 4)(s + 0.05)}{s^2} \tag{4}$$

The Bode plot with robustness margins is shown in Fig. 2. From this diagram it can be seen how the gain margin remains infinite as in the PI controller, while the phase margin obtained a value of 90.2 °. It is important to highlight that the only design parameter that was necessary to modify was the bandwidth, which was increased to 10.1 rad / s, this is because the gain necessary to maintain the original bandwidth greatly reduced the integral effect of the controller, therefore, it was necessary to increase the gain so that the integral effect was preserved, and the bandwidth did not change noticeably.

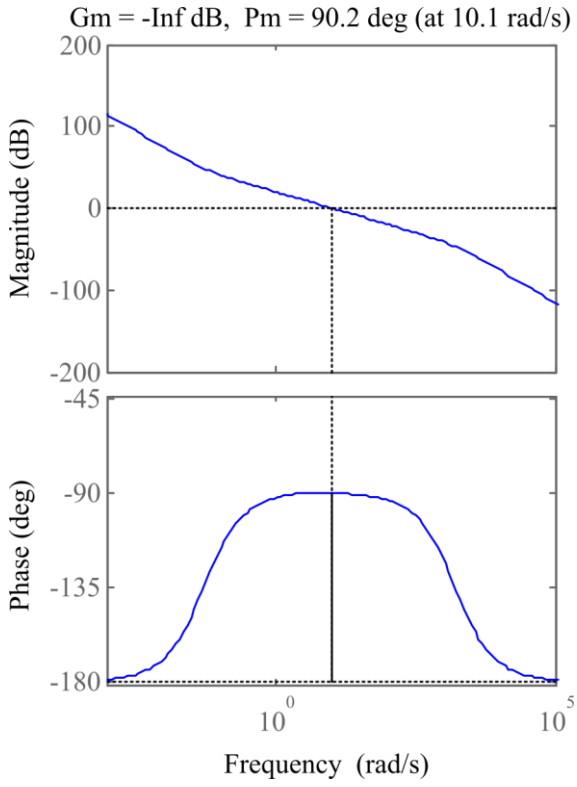

Fig. 2. PII Control system Bode diagram.

3.1 PII Simulations

To test the performance of the PII controller, the motor is run at low speeds in regulation and the responses are compared with those obtained with the PI controller. For the first test a reference signal is applied at -500 to 500rpm, the comparative graphs are shown in Fig. 3 to 6.

From this test, in Fig.3, it is observed how in the speed responses, there is a dead zone at the beginning of the simulation, which for the case of the PI controller lasts 0.3 seconds, while for the PII the time is reduced to 0.2 seconds, the errors obtained by the controllers are 0.9% for the PII and 0.01% for the PI. In addition, it is appreciated how the PII controller eliminate the dead zone of the motor, while the PI continues to show this phenomenon. Note that in the second cycle of the reference signal the PI control shows a greater dead zone, this can be due to several factors, mainly speed or position. In the case of this last factor, it affects the inductance and therefore the torque. For this reason, it is possible that the dead zone phenomenon may affect the motor differently depending on these factors and independently of the controller applied to the motor. In Fig. 4 it can be seen how the control input rises with greater speed in the case of the PII, for this reason the motor reaches the reference faster than in the case of the PI control, subsequently both responses are established at the same voltage.

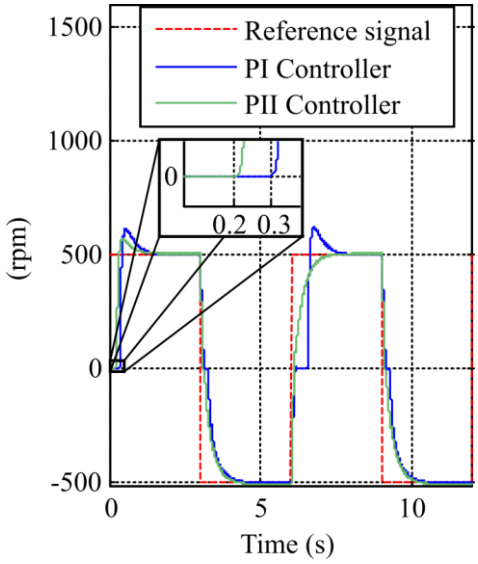

Fig 3. Rotor´s speed response to reference signal from -500 to 500 rpm.

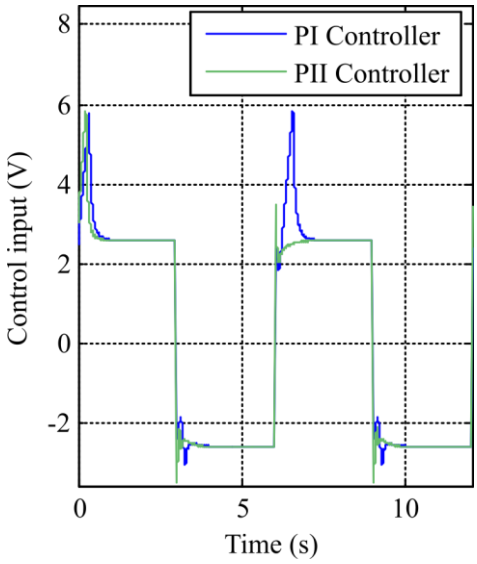

Fig. 4. Control input response to reference signal from -500 to 500 rpm.

In the case of torque and phase currents, Figs. 5 and 6, the responses of the PII follow a behavior very similar to the responses of the PI, with the fundamental difference that the responses of the first are established earlier.

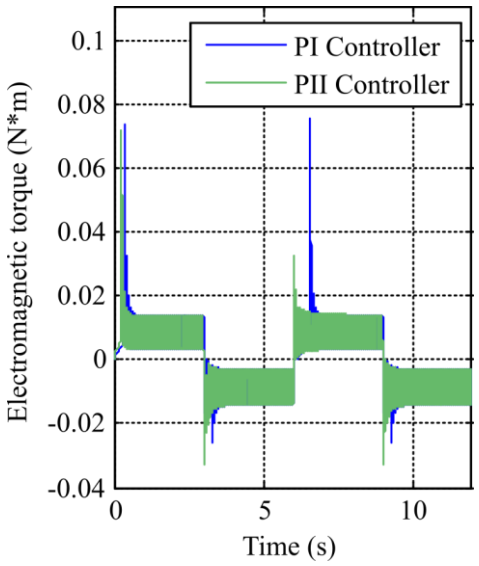

Fig. 5. Torque response to reference signal from -500 to 500 rpm.

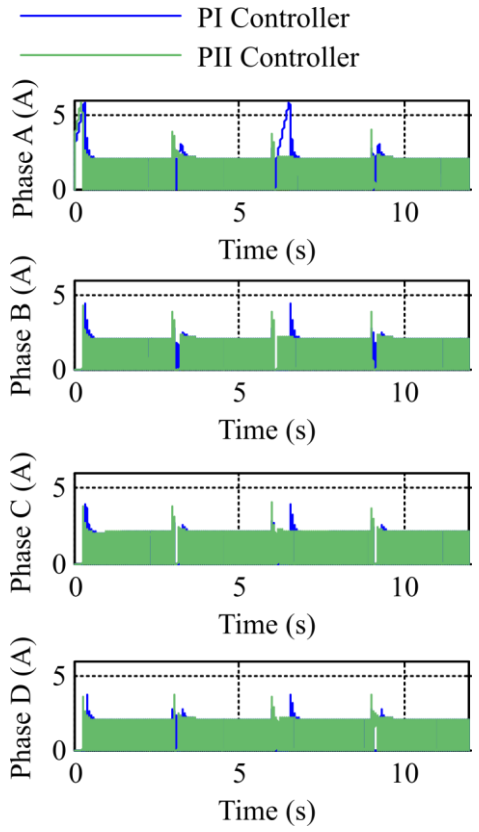

Fig. 6. Phase currents responses to reference signal from -500 to 500 rpm.

As a last test, the reference value is changed, so that the motor is required to operate between -200 and 200 rpm, the responses obtained are shown in Fig. 7 to 10.

In Fig. 7 it is observed how again the PII controller establish the motor in less time than the PI, obtaining 0.46 and 0.63 seconds correspondingly.

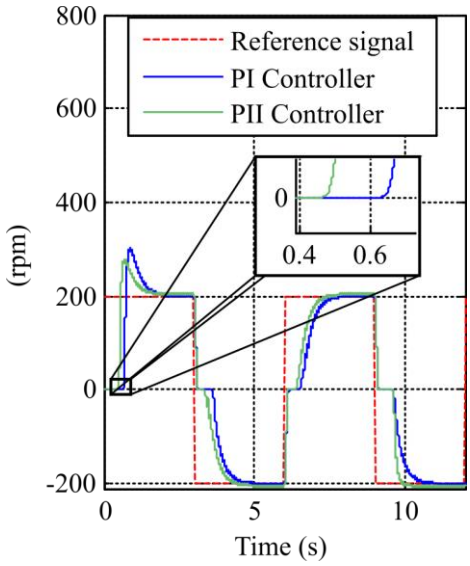

Fig 7. Rotor´s speed response to reference signal from -200 to 200 rpm.

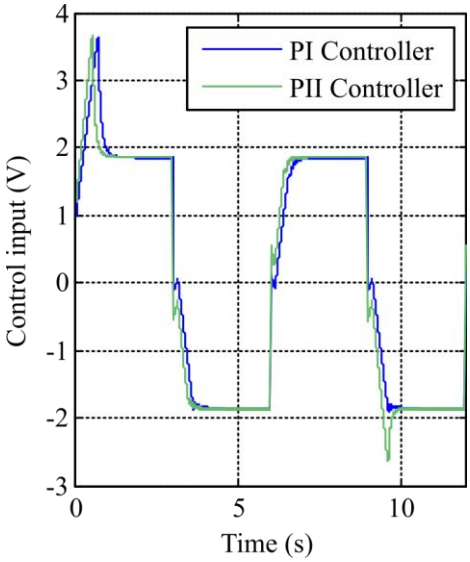

Fig. 8. Control input response to reference signal from -200 to 200 rpm.

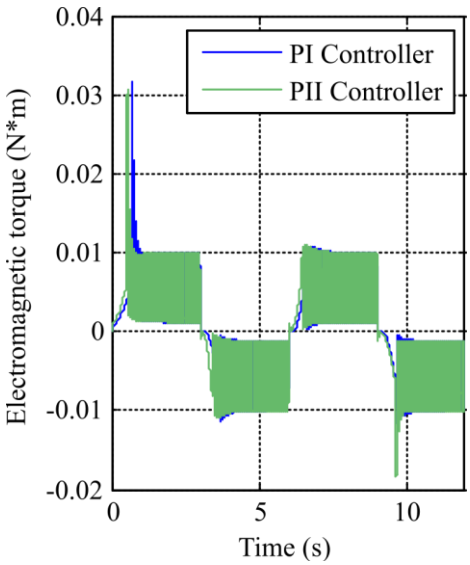

Fig. 9. Torque response to reference signal from -200 to 200 rpm.

However, the PII controller gets a 1.7% error, while the PI gets a 0.05% error. In addition, as mentioned in the previous test, it is possible the appearance of dead zones such as the one that occurred between seconds 9.1 and 9.6, where both controllers showed a dead zone of similar duration, again this occurs because the behavior of the motor depends on largely on speed and position conditions.

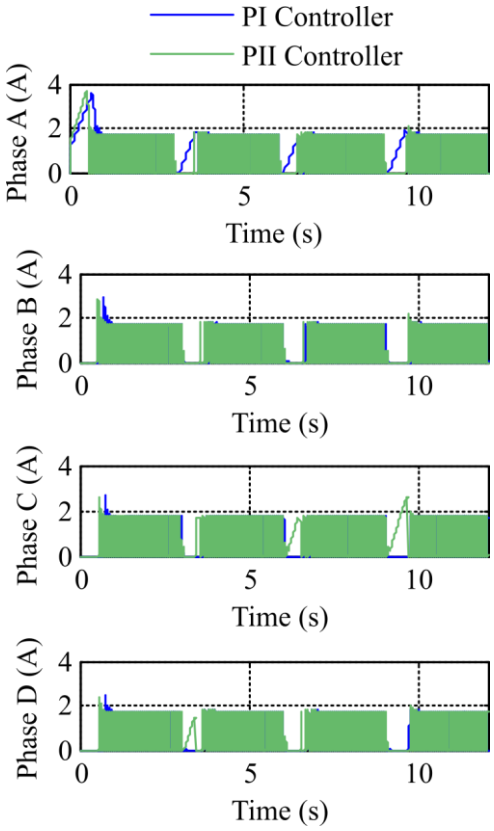

Fig. 10. Phase currents responses to reference signal from -200 to 200 rpm.

In the case of the control input responses, torque and phase currents, Fig.8, 9 and 10, those show a behavior like those obtained in the previous test. Based on the results obtained from the previous tests, it is observed that indeed the PII controller showed a better performance when dealing with the dead zone phenomenon, reducing this by at least 27% at startup and in some cases, in full operation, the dead zone was reduced in its entirety as observed in Fig. 9.2. As expected, the lower the operating speed the more difficult it is to deal with the dead zone.

4 Proposed PI+RR Controller

One of the main characteristics of the switched reluctance motor is the oscillations or ripple in the torque and speed responses, which is an undesirable characteristic since these oscillations can cause mechanical vibrations and even audible noise, as well as poor regulation performance. For this reason, in this section we propose a technique to reduce the ripple, which consists in assuming that the ripple of the speed response is noise located at the input of the motor *G(s)*, as observed in Fig. 11, which is represented by δ. The technique shown in this section was named Ripple Reductor (RR), it is based on noise reduction disturbance observers (NR-DOB) [19].

This technique is responsible for reducing sensor noise and low-frequency noise while RR focuses on reducing high-frequency ripple.

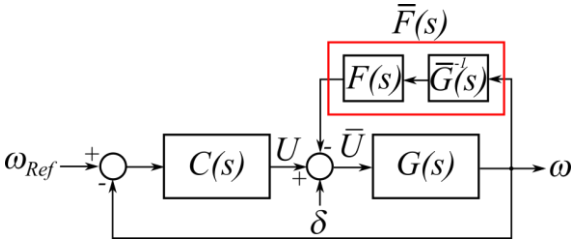

Fig. 11 PI+ Ripple Reductor Controller Block Diagram

It is desired to achieve is $\bar{U}=U$, for this it is necessary to recover the noise from the output ω, to do the latter ω is passed through a filter $\bar{F}(s)$ formed by the inverse function of the model of the motor $\bar{G}^{-1}(s)$ and *F(s)*, which together must be causal to guarantee that it is implementable. The filter $\bar{F}(s)$ is of the band pass type with *K* gain and lower and upper frequencies ω_{f1} and ω_{f2} respectively. Calculating the transfer functions ω/ω_{Ref} and ω/δ; (5) and (6).

$$\frac{\omega}{\omega_{Ref}}(s)=\frac{CG}{1+FG\bar{G}^{-1}+CG} \tag{5}$$

$$\frac{\omega}{\delta}(s)=\frac{G}{1+FG\bar{G}^{-1}+CG} \tag{6}$$

Analyzing (5) and (6), inside and outside the filter band, the following is obtained (7) and (8).

$$\begin{aligned} &Si\ \ \omega_{f1}<\omega<\omega_{f2} \ \Rightarrow\ |F|\approx K \\ &\Rightarrow\ \frac{\omega}{\omega_{Ref}}(s)\approx\frac{CG}{1+K+CG} \\ &Si\ \ \omega\notin(\omega_{f1},\omega_{f2}) \ \Rightarrow\ |F|\approx 0 \\ &\Rightarrow\ \frac{\omega}{\omega_{Ref}}(s)\approx\frac{CG}{1+CG} \end{aligned} \tag{7}$$

$$Si \ \ \omega_{f1} < \omega < \omega_{f2} \ \Rightarrow \ |F| \approx K$$
$$\Rightarrow \ \frac{\omega}{\delta}(s) \approx \frac{G}{1+K+CG} \approx \frac{G}{1+K}$$
$$Si \ \ \omega \notin (\omega_{f1}, \omega_{f2}) \ \Rightarrow \ |F| \approx 0 \qquad (8)$$
$$\Rightarrow \ \frac{\omega}{\delta}(s) \approx \frac{G}{1+CG}$$

From (7) it is observed that within the filter frequency band, the control system has a small deterioration due to the denominator, very similar to the expected behavior of the closed loop of any control system. This behavior if you get out of the frequency band. Therefore, the behavior of the control system remains very similar to normal. On the other hand, the behavior of the system with respect to noise, within the band, the attenuation of the noise is directly affected by the motor itself, since the controller at these frequencies has a gain of approximately 0. Outside the frequency band, particularly at low frequencies, the behavior of the system with respect to noise tends to zero, since the controller has great gain at these frequencies, this is the case of the frequencies of the reference signal. It is important to highlight that, to guarantee internal stability, as can be seen in (5) and (6), the motor model $\bar{G}$ must be stable and with minimum phase, therefore, the motor must also comply with these characteristics.

The design of the *F(s)* filter consists of a derivative or zero at frequency 0 and four poles, the first pole is placed one decade before the ripple frequency while the other three are placed at a frequency greater than one decade later. For $\bar{G}^{-1}(s)$ the transfer function of (1) is taken. The frequency of the ripple is calculated as the product of the number of commutations of the motor per revolution, multiplied by the angular frequency of the rotor; (9), for this filter the nominal speed was selected.

$$f_{rizo} = 24 f_{rotor} \Rightarrow f_{rizo} = 5026.6 rad/s; \qquad (9)$$

The transfer function obtained for the filter *F(s)* is shown in (10), while its Bode diagram is shown in Fig. 12

$$F(s) = \frac{0.007s}{(s+500)(s+60000)(s+70000)(s+100000)} \qquad (10)$$

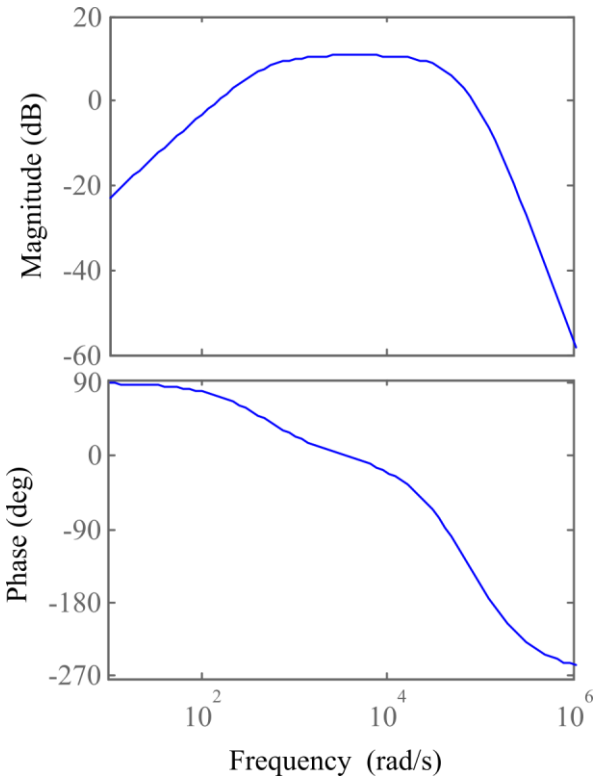

Fig. 12. Filter *F(s)* Bode diagram.

4.1 PII Simulations

To test this technique, two tests were carried out, where the control system is subjected to regulation, first a square signal is given as a reference signal oscillating between 1500 and 2500rpm, to observe the behavior of the motor, just around the operating point, the Control system responses are shown in Figs. 13 to 16.

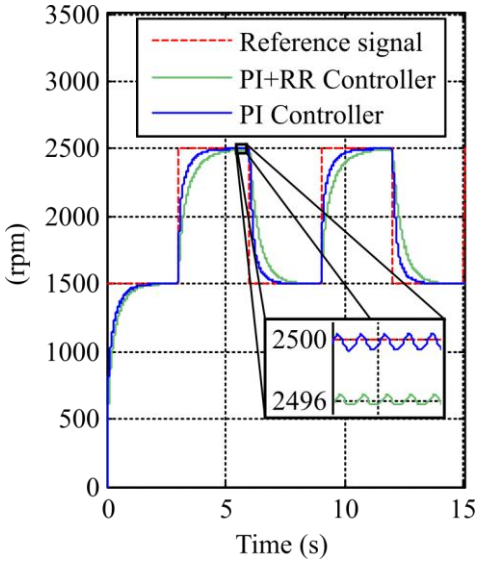

Fig 13. Rotor´s speed response to reference signal from 1500 to 2500 rpm.

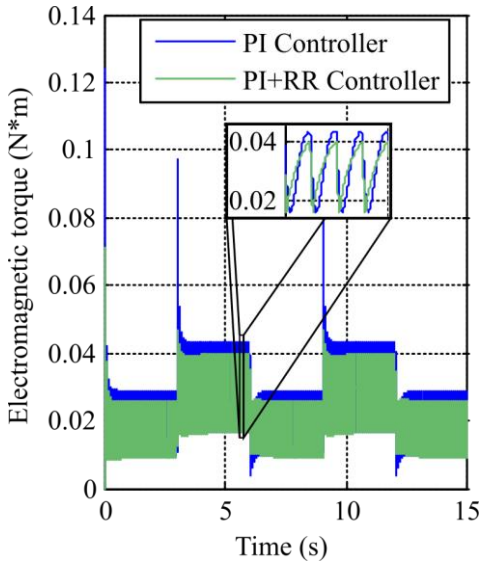

Fig. 14. Torque response to reference signal from 1500 to 2500 rpm.

In Fig. 13 it is observed how the speed response of the PI+RR control is established at the reference speed with a minimum error and obtains a 0.05% of ripple while the PI ripple has a value of 0.08% Therefore, the ripple reduction is 37.5% for speeds of 1500rpm. As for speeds of 2500rpm, the ripple values of 0.03% and 0.04% for the PI+RR and PI respectively, with a reduction of 25%.

For the case of the torque response, Fig. 14, the ripple obtained was 80.7% for the PI+RR and 92.7% with a reduction of 12.9% for speeds of 500 rpm while for speeds of 2500 rpm the data obtained, they were 75.8%, 87.1% and 13%.

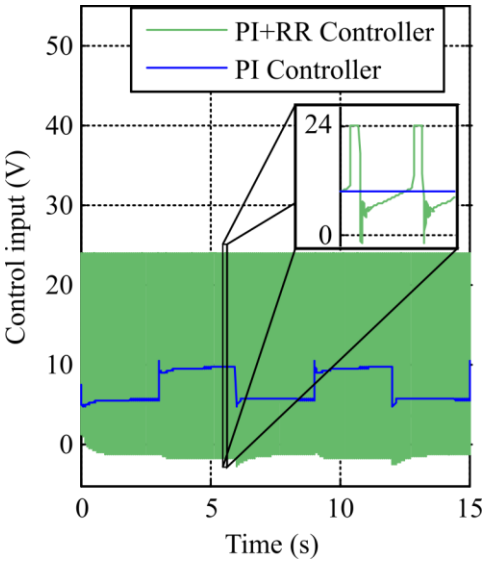

Fig. 15. Control input response to reference signal from 1500 to 2500 rpm.

In Fig. 15 it is observed how the control input signal of the PI + RR control is notably different from that obtained from the PI; this is because the PI + RR control needs to apply high frequency input voltages to the motor as large as possible to be able to counteract high frequency ripple speed fluctuations. As can be seen in this same figure, the maximum value is limited to 24V, to protect the motor and keep it in normal operation.

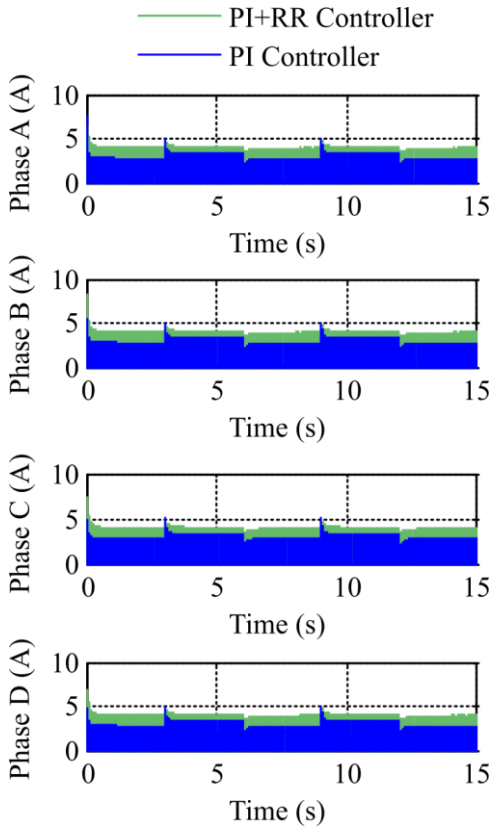

Fig. 16. Phase currents responses to reference signal from 1500 to 2500 rpm.

Finally, in Fig. 16, the current responses maintain a very similar average value in both control systems, with a subtle change in the shape of the peaks, caused by the sudden voltage changes of the control input.

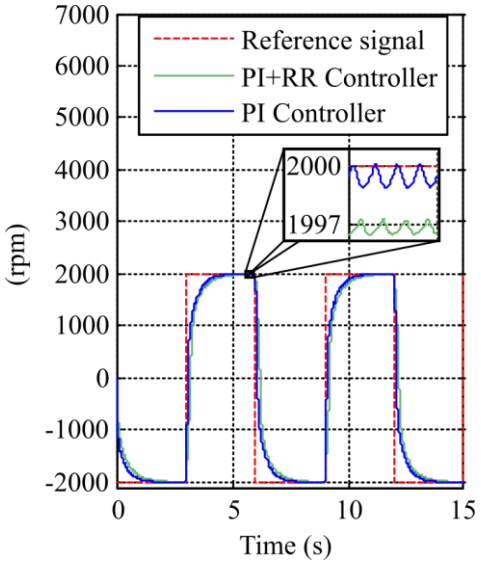

Fig 17. Rotor´s speed response to reference signal from -2000 to 2000 rpm.

For the next test the reference signal ranges between -2000 and 2000rpm, once again the responses of both control systems are shown below, in Figs. 17 to 20.

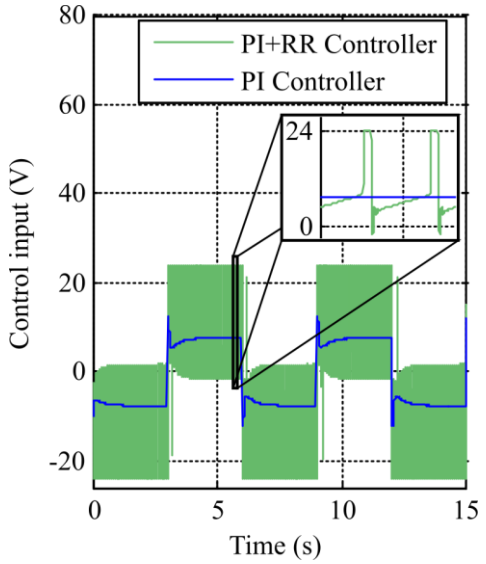

Fig. 18. Control input response to reference signal from -2000 to 2000 rpm.

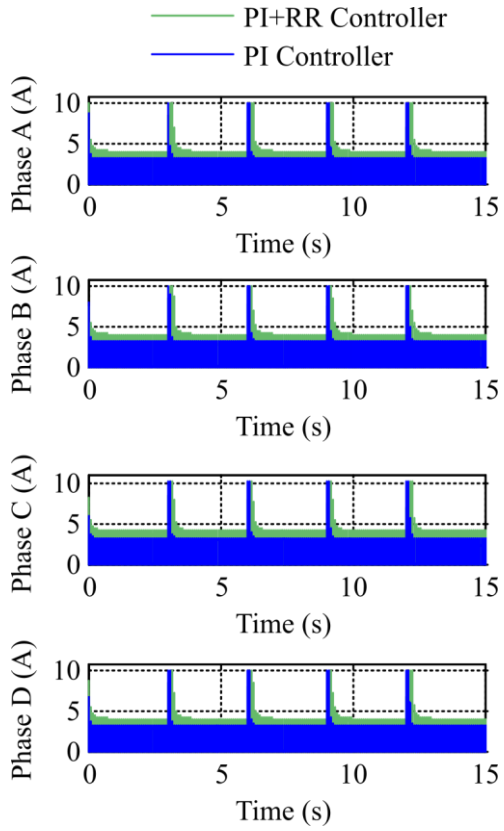

Fig. 19. Phase currents responses to reference signal from -200 to -200 rpm.

The behavior of both control systems is similar to that shown in the previous test, with only minimal changes. The results of ripple reduction in speed and torque are summarized in Table I.

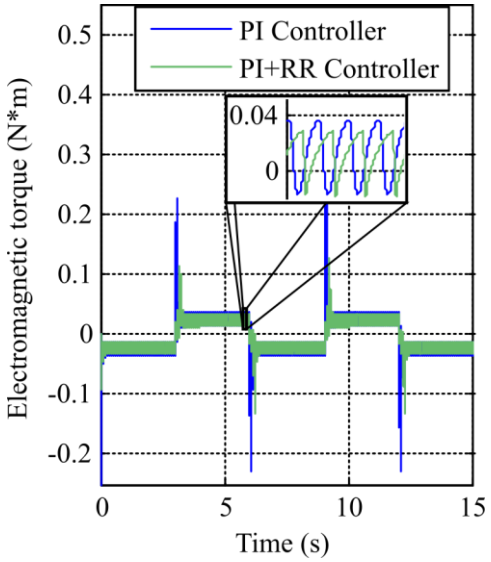

Fig. 20. Torque response to reference signal from -2000 to 2000 rpm

TABLE I RIPPLE REDUCTION PERCENTAGE AROUND THE OPERATING POINT

Rotor's speed (rpm)	Ripple reduction of ω (%)	Ripple reduction of τ_e (%)
1500	37.5	12.9
2000	33.3	14.4
2500	25	13

5 Conclusion

In this article, two solutions based on classical control strategies were presented in order to reduce two undesirable effects which usually appear in the speed response of any SRM known as ripple and dead zone. The simulations shown in this work are based on the simplified model of an SRM 8/6, which includes the non-linear model of Coulomb friction plus viscous friction and an ideal inverter circuit. The first controller shown is the PII controller from whose tests it is observed how this manages to reduce the time that the dead zone lasts by at least 27%, with respect to what was obtained from the PI controller. However, the PII controller obtains a steady state error greater than that obtained from the PI controller, this error increase is 1.65% in the worst case. On the other hand, the second controller presented was the PI + RR controller, in which the tests carried out showed that this controller manages to reduce the speed ripple magnitude by at least 25%, while in the case of torque the reduction obtained was 13%. The problem with the use of this control is that, when trying to reduce the rapid oscillations of the torque, the controller compensates for this by applying voltages as large as possible with very high frequency according to ripple frequency, for this reason, it was necessary to limit the supply voltage range of the

drive motor. -24 to 24V, this can cause the motor to operate in its saturation region, therefore, it is necessary to use a model that contemplates this phenomenon for its correct simulation.

From both the PII and PI + RR control tests, it is concluded that although both controllers met their respective dead zone and ripple reduction objectives, they are not worth using them since their main application is within a region of low speeds, since, within this region, both the dead zone and the ripple are greater and can represent a problem for the motor user. It must be considered that one of the advantages of these motors is their high speed, therefore, their application is found in regions with higher speeds.

References:

[1] K. Kiyota, T. Kakishima, and A. Chiba, "Comparison of test result and design stage prediction of switched reluctance motor competitive with 60 kw rare-earth pm motor," *IEEE Transactions on Industrial Electronics*, vol. 61, no. 10, pp. 5712-5721, 2014.

[2] T. J. E. Miller, *Electronic control of switched reluctance machines.* Elsevier, 2001.

[3] A. E. Fitzgerald, C. Kingsley, S. D. Umans, and B. James, *Electric machinery*. McGraw-Hill New York, 2003, vol. 5.

[4] R. Krishnan, *Switched reluctance motor drives: modeling, simulation, analysis, design, and applications*. CRC press, 2017.

[5] P. F. Portells, "Diseño de un accionamiento de reluctancia autoconmutado orientado al control de par," *SRM*, vol. 8, p. 6, 2013.

[6] L. Liu, M. Zhao, X. Yuan, and Y. Ruan, "Direct instantaneous torque control system for switched reluctance motor in electric vehicles," *The Journal of Engineering*, vol. 2019, no. 16, pp. 1847-1852, 2019.

[7] S. Wang, Z. Hu, and X. Cui, "Research on novel direct instantaneous torque control strategy for switched reluctance motor," *IEEE Access*, vol. 8, pp. 66 910-66 916, 2020.

[8] K. Aiso and K. Akatsu, "High speed SRM using vector control for electric vehicle," *CES Transactions on Electrical Machines and Systems*, vol. 4, no. 1, pp. 61-68, 2020.

[9] M. Ma, Z. Wang, Q. Yang, S. Yang, and X. Zhang, "Vector control strategy of a t-type three-level converter driving a switched reluctance motor," *Chinese Journal of Electrical Engineering*, vol. 5, no. 4, pp. 15-21, 2019.

[10] H. Haq and H. I. Okumus, "Flc-dtc method for torque ripples minimization of 8/6 switched reluctance motors drive," *JAREE (Journal on Advanced Research in Electrical Engineering)*, vol. 4, no. 1, 2020.

[11] A. Uysal, S. Gokay, E. Soylu, T. Soylu, and S. Çaşka, "Fuzzy proportional-integral speed control of switched reluctance motor with matlab/simulink and programmable logic controller communication," *Measurement and Control*, vol. 52, no. 7-8, pp. 1137-1144, 2019.

[12] Z. Wei, M. Zhao, X. Liu, and M. Lu, "Speed control for srm drive system based on switching variable proportional desaturation pi regulator," *IEEE Access*, vol. 9, pp. 69 735-69 746, 2021.

[13] N. Saha and S. Panda, "Speed control with torque ripple reduction of switched reluctance motor by hybrid many optimizing liaison gravitational search technique," *Engineering science and technology, an international journal*, vol. 20, no. 3, pp. 909-921, 2017.

[14] G. A. A. Aziz and M. Amin, "High-precision speed control of four-phase switched reluctance motor fed from asymmetric power converter," in *2017 Intl Conf on Advanced Control Circuits Systems (ACCS) Systems & 2017 Intl Conf on New Paradigms in Electronics & Information Technology (PEIT)*. IEEE, 2017, pp. 297-304.

[15] J. D. González-San Román, J. U. Liceaga-Castro, I. I. Siller-Alcalá and E. Campero-Littlewood, "Structural analysis of 8/6 switched reluctance motor linear and non-linear models," *International Journal of Circuits, Systems and Signal Processing,* vol. 15, pp. 1464-1474, 2021.

[16] K. Ogata, *Ingeniería de control moderna.* Pearson Educación, 2010, vol. 5.

[17] . D. González-San Román, J. U. Liceaga-Castro, I. I. Siller-Alcalá and E. Campero-Littlewood, "Performance tests of a PI speed controller applied in a non-linear model of a switched reluctance motor 8/6," *Transactions on Systems and Control,* vol. 16, pp. 508-518, 2021.

[18] C. A. Pérez-Gómez, J. U. Liceaga-Castro, and I. I. Siller-Alcalá, "Comparative study between classical controllers and inverse dead zone control for position control of a permanent magnet dc motor with dead zone," in *Transactions on Power Systems*, vol. 15. WSEAS, 2020.

[19] J. U. Liceaga-Castro, I. I. Siller-Alcalá, and E. Liceaga-Castro, "Noise reduction disturbance observer global stability and robustness conditions based on the nyquist stability criteria," *International Journal of Engineering Research and Development*, vol. 14, 2020.

Contribution of individual authors to the creation of a scientific article

Jesús D. González-San Román programmed the models, carried out the simulations and contributed to the theoretical analysis and design of the controllers.
Jesús U. Liceaga-Castro and Irma I. Siller-Alcalá contributed to the theoretical analysis and design of the controllers.
Roberto A. Alcantara-Ramirez carried out the electrical motor's analysis.

Sources of funding for research presented in a scientific article or scientific article itself

The project was funded by the UAM-Azc and by CONACYT scholarship grant to Jesús D. González-San Román

Creative Commons Attribution License 4.0 (Attribution 4.0 International , CC BY 4.0)